JOURNAL OF GEOPHYSICAL RESEARCH, VOL. 102, NO. A7, PAGES 14,141–14,148, JULY 1, 1997

Recurrent geomagnetic storms and relativistic electron enhancements in the outer magnetosphere: ISTP coordinated measurements

D.N. Baker,[1] X. Li,[1] N. Turner,[1] J.H. Allen,[2] L.F. Bargatze,[3,4] J.B. Blake,[5] R.B. Sheldon,[6] H.E. Spence,[6] R.D. Belian,[7] G.D. Reeves,[7] S.G. Kanekal,[8] B. Klecker,[9] R.P. Lepping,[10] K. Ogilvie,[10] R.A. Mewaldt,[11] T. Onsager,[12] H.J. Singer,[12] and G. Rostoker[13]

Abstract. New, coordinated measurements from the International Solar-Terrestrial Physics (ISTP) constellation of spacecraft are presented to show the causes and effects of recurrent geomagnetic activity during recent solar minimum conditions. It is found using WIND and POLAR data that even for modest geomagnetic storms, relativistic electron fluxes are strongly and rapidly enhanced within the outer radiation zone of the Earth's magnetosphere. Solar wind data are utilized to identify the drivers of magnetospheric acceleration processes. Yohkoh solar soft X-ray data are also used to identify the solar coronal holes that produce the high-speed solar wind streams which, in turn, cause the recurrent geomagnetic activity. It is concluded that even during extremely quiet solar conditions (sunspot minimum) there are discernible coronal holes and resultant solar wind streams which can produce intense magnetospheric particle acceleration. As a practical consequence of this Sun-Earth connection, it is noted that a long-lasting E>1MeV electron event in late March 1996 appears to have contributed significantly to a major spacecraft (Anik E1) operational failure.

Introduction

Large, nonrecurrent geomagnetic storms develop at Earth due to aperiodic solar disturbances. One of the most notable such features of solar activity is coronal mass ejections (CMEs). These are large expulsions of material from the Sun [e.g., *Gosling et al.*, 1991, references therein] which are normally associated with eruptive prominences and other solar disturbances. It is sometimes found that the leading edges of CMEs are moving outward from the sun at a speed much higher than that of the normal solar wind. Thus these fast CMEs can appear as large plasma structures, or plasmoids, moving rapidly through the heliosphere. Their outward motion can lead to great distortion of the ambient interplanetary medium and, given a sufficiently high relative speed, CMEs can be drivers for strong interplanetary shock waves.

Gosling et al. [1991] discussed CMEs as plasma structures with closed field line topology. Rapid motion through the ambient solar wind would lead to a forward shock wave in front of the CME. The ambient interplanetary magnetic field (IMF) that is draped over (and under) the body of the CME causes strong northward or southward IMF ahead of the CME. The field compression and draping would lead to stronger than normal magnetic fields at the leading edge of the structure and, of course, the plasma flow velocity would also be high. This would produce a geomagnetic storm characterized by a large field compression and distortion as the CME and associated shock wave impact the Earth's magnetosphere.

In contrast to major storms (defined here to be when the global geomagnetic index Ap is greater than 70), weaker geomagnetic storms (with peak Ap in the range 20-50) are typically driven by high-speed solar wind streams that are characteristic of solar minimum conditions. These streams are thought to originate in solar coronal holes. Generally, transequatorial coronal holes are well developed in the declining phase of the solar cycle rather than right at sunspot minimum. In cycle 22, the best developed coronal holes were seen to recur between 1993 and 1995. Nonetheless, we will present evidence of coronal holes in early 1996 and will also show high-speed solar wind measured at 1 AU. Long-term observations in the outer magnetosphere (L~6.6) demonstrate that energetic electron fluxes are strongly modulated by solar wind streams [*Baker et al.*, 1986, 1994a]. Lower-energy ($\lesssim$ 300 keV) particle fluxes track the solar wind varia-

[1]Laboratory for Atmospheric and Space Physics, Campus Box 590, University of Colorado, Boulder, CO 80303-0590.
[2]SCOSTEP Secretariat, NOAA/NGDC, Boulder, CO 80302.
[3,4]Department of Physics, Montana State University, Bozeman, MT 59717-0350.
[5]Aerospace Corp., Los Angeles, CA 90009.
[6]Center for Space Physics, Boston University, Boston, MA 02215.
[7]Los Alamos National Laboratory, Los Alamos, NM 87545.
[8]Huges/STX, NASA Goddard Space Flight Center, Greenbelt, MD 20771.
[9]Max Planck Institut für Physik und Astrophysik, D-8046 Garching Bei Muchen, Germany.
[10]NASA Goddard Space Flight Center, Greenbelt, MD 20771.
[11]California Institute of Technology, Pasadena, CA 91125.
[12]Space Environment Center, NOAA R/E/SE, 325 Broadway, Boulder, CO 80302.
[13]Department of Physics, University of Alberta, Edmonton, Alberta, Canada.

Paper number 97JA00565.
0148-0227/97/97JA-00565$09.00

tions quite closely and appear to be the direct product of magnetospheric substorm activity (which is obviously controlled by the solar wind and the IMF). Higher-energy (>300 keV) particle fluxes are also modulated by the solar wind streams but are not directly related to substorm acceleration mechanisms. In fact, the highest-energy electrons show strong recurrence tendencies at the 27-day rotation period of the Sun [*Williams*, 1966; *Paulikas and Blake*, 1979]. These appear to closely parallel "recurrent" geomagnetic storms, so it is important from a physical point of view to understand these phenomena.

Given the intense interest in understanding the acceleration and transport of high-energy magnetospheric particles and their dependence on solar and magnetospheric conditions, data in the early part of 1996 from several scientific and operational spacecraft have been used to examine global solar-terrestrial connections. These data are employed to provide a broad context for simultaneously observing the changes occurring at the Sun, in the interplanetary medium, and in the geospace environment under solar minimum conditions. The ISTP spacecraft armada and coordinated ground-based measurements yield a comprehensive view of the complex processes that modulate energetic charged particles in the magnetosphere; the importance of these particles is underscored in this study through the possible association of a major satellite failure with the radiation environment within which it was operating.

Observations

Figure 1 shows the daily *Ap* geomagnetic index values [*Mayaud*, 1980] for the first three months of 1996. Small, recurrent storms with peak *Ap* activity levels in the range of 20-40 are evident. The *Ap* enhancements peak every 12-15 days. The overall pattern is one of relatively weak activity with no major storms during the interval. The largest event (*Ap* = 38) occurred on day 81 (March 21).

In the present era, since the launch of the WIND spacecraft in November 1994, we are fortunate to have nearly continuous solar wind data. Figure 2a shows the solar wind

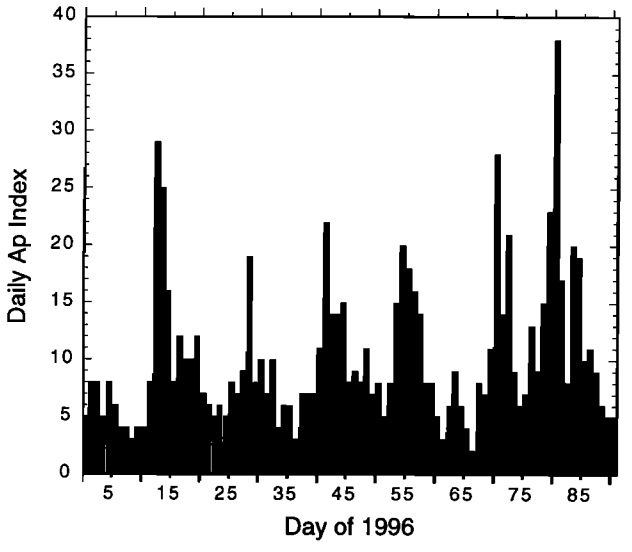

Figure 1. Daily *Ap* magnetic index data for the first 3 months of 1996.

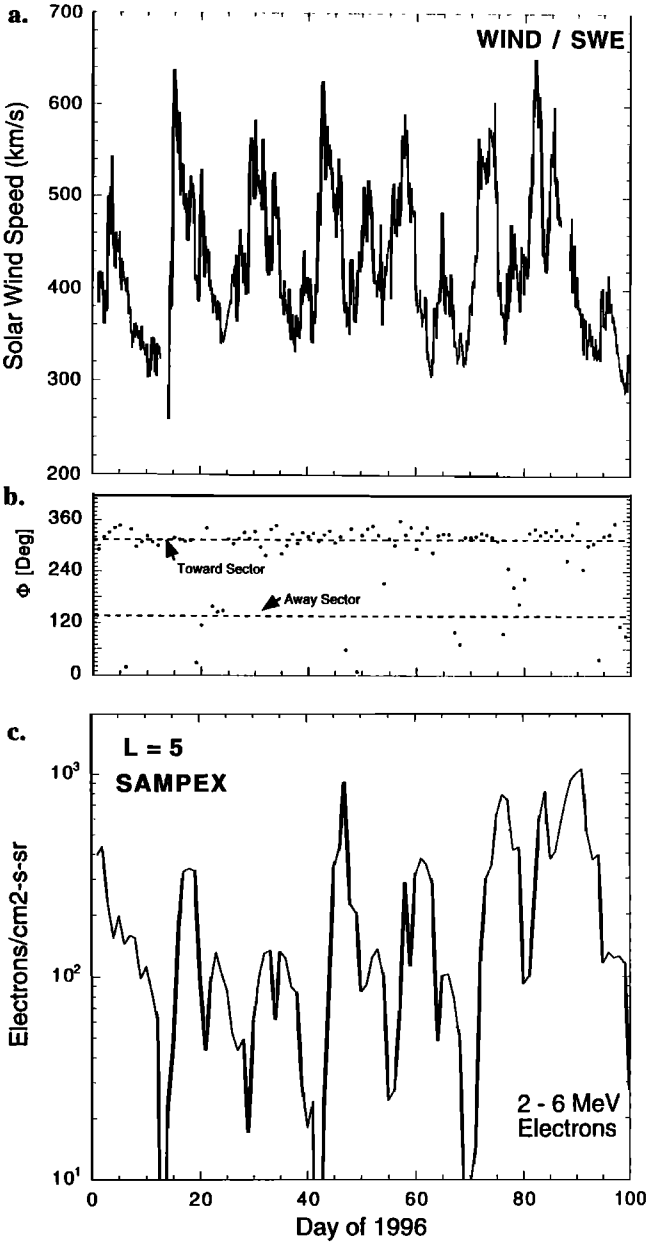

Figure 2. (a) The solar wind speed measured by WIND, while the (b) GSM longitude of the IMF measured by WIND. The IMF was in a "toward" sector configuration for most of this period. (c) Daily-average fluxes of 2-6 MeV electrons at *L*=5 from the PET sensor on SAMPEX.

speed (V_{SW}) measured by the Solar Wind Experiment (SWE) onboard WIND [*Ogilvie et al.*, 1995]. Data are shown as hourly averages for day 1 (January 1) to day 100 (April 9) of 1996. It is evident from Figure 2a that there were several strong solar wind stream events throughout early 1996. Notable examples of solar wind speed peaks include those occurring on days ~15, ~28, ~42, ~57, ~72, and ~82. Obviously, there were "recurrent" streams that were associated with the 27-day solar rotation period: The interleaving of two sets of such recurrent streams produced an ~13-day stream enhancement periodicity. The measured IMF sector structure using WIND data is shown as a separate panel in Figure 2.

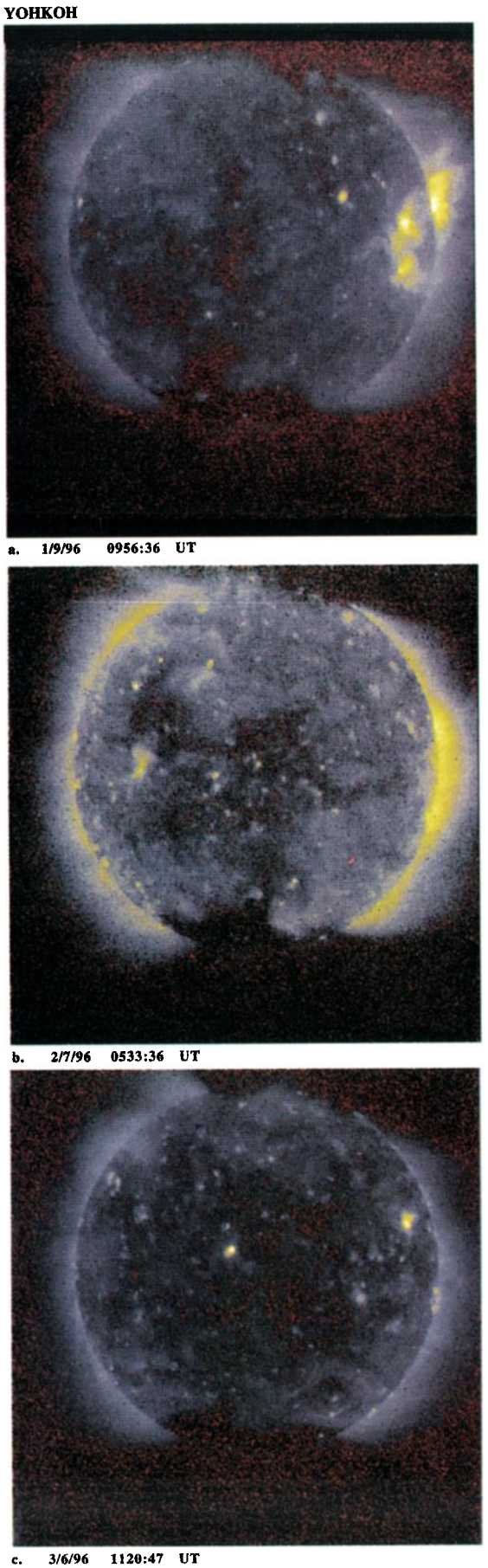

Figure 2c shows 2-6 MeV electron intensities measured by the Solar, Anomalous, and Magnetospheric Particle Explorer (SAMPEX) spacecraft at low-Earth, polar orbit [see *Baker et al.*, 1993]. A subset of the Proton-Electron Telescope (PET), [see *Cook et al.*, 1993] data averaged each day for L=5 (±0.1) is plotted for the period day 1 to day 100 of 1996. The SAMPEX data show relatively brief flux peaks associated with solar wind streams in January and February, but the larger and longer lasting flux enhancement of late March is quite clear. The occurrence of relativistic electron enhancements associated with solar wind streams (but delayed by some days) has been known for some time [e.g., *Paulikas and Blake*, 1979]. The exact mechanism, however, for the electron acceleration process remains a topic of intensive research. It appears that the direction of the IMF and the pattern of solar wind speed changes combine to play a determining role [*Blake et al.*, 1997].

Given the well-known result that the largest solar wind streams originate from solar coronal holes [e.g., *Feldman et al.*, 1978], available solar soft X-ray (Yohkoh) and extreme ultraviolet (SOHO) data have been examined to identify solar wind stream source regions. Plate 1a shows a Yohkoh soft X-ray image of the sun taken at 0956:36 UT on January 9, 1996. In general, the solar corona was seen in Yohkoh data to be extremely quiet and unstructured during the early part of 1996. However, a large coronal hole at low solar latitudes is evident near central meridian on January 9. This hole undoubtedly gave rise to the solar wind stream which the Earth encountered on January 14 (see Figure 2a). This same coronal hole was seen to return in early February and again in early March of 1996 as shown in the Yohkoh images of Plates 1b and 1c. (Note that *Baker et al.* [1996] also showed SOHO/EIT data which confirmed the identification of these coronal hole features seen in Yohkoh data).

A key to producing enhanced geomagnetic activity and subsequent relativistic electron events within the magnetosphere is a combination of high-speed solar wind and strongly southward IMF. Figure 3 shows in the center panel the solar wind speed from day 60 through day 100. The lower panel shows the concurrent values of solar wind number density. In the upper panel are shown hourly averages of the IMF north-south component (B_z) in GSM coordinates for days 75-86. The IMF data were obtained with the magnetic field investigation (MFI) onboard the WIND spacecraft [*Lepping et al.*, 1995]. It is seen that the IMF was rather strongly and persistently southward from day 77 (March 17) to near the end of day 81 (March 21). This negative B_z was "piled up" at the leading edge of the high-speed solar wind stream which reached the Earth's vicinity on ~day 80 (March 20). As seen in Figure 1, the southward IMF and high value of V_{SW} produced a notable increase in the global magnetic index Ap. The Ap value peaked on March 21 when the IMF was most negative.

Plate 1. (a) A soft X-ray image of the Sun (courtesy of L. Acton) taken by the Yohkoh spacecraft at 0956:36 UT on January 9, 1996. A coronal hole is seen near central meridian extending from the south polar region across the equatorial plane. (b) Similar to Figure 3a but for February 7, 1996. (c) Similar to Figure 3a but for March 6, 1996.

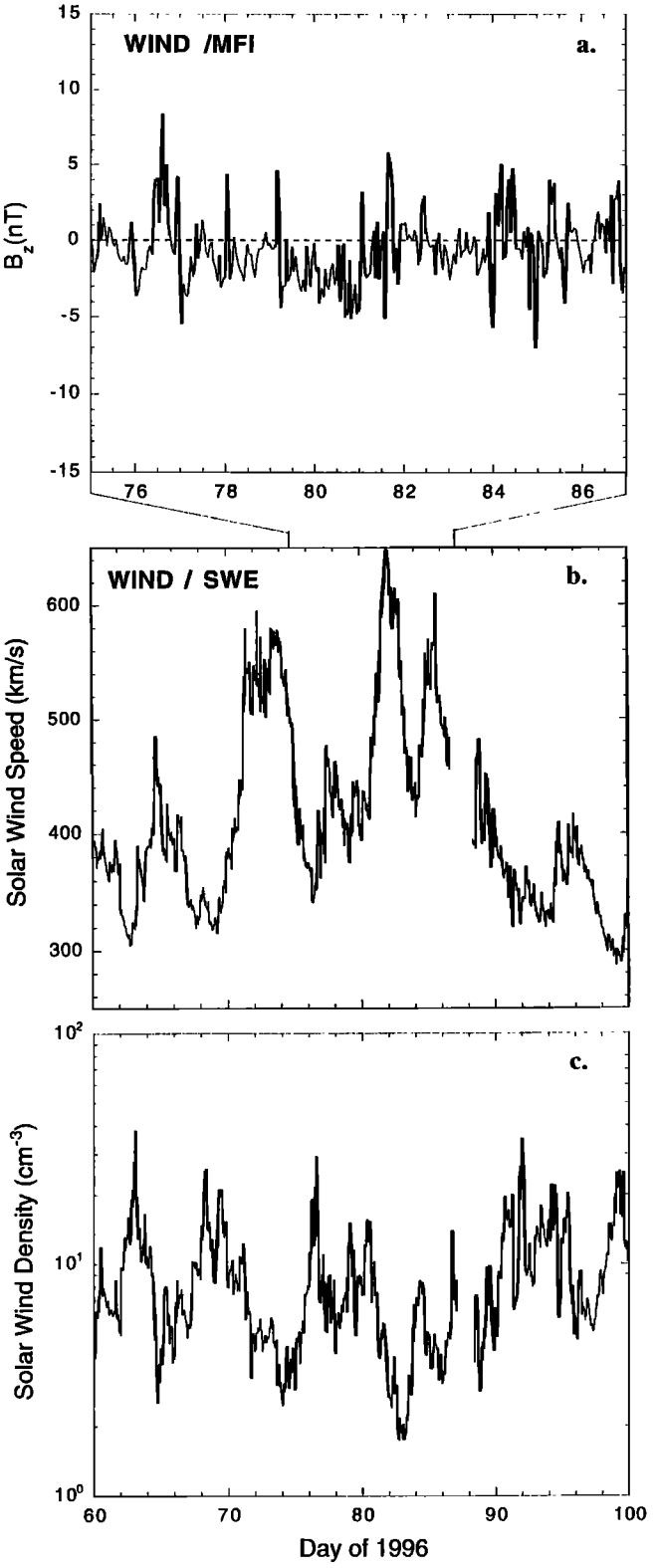

Figure 3. (a) Hourly averages of the interplanetary magnetic field B_z component for days 75-86. (b) Hourly averages of solar wind speed for days 60-100 of 1996. (c) Hourly averages of solar wind density for days 60-100 of 1996.

In Figure 4, data from the geostationary orbit GOES 8 spacecraft are shown for electrons with E>2MeV. Note that the GOES data are shown as daily fluences. Looking at the low-frequency temporal patterns, it is seen from Figure 4

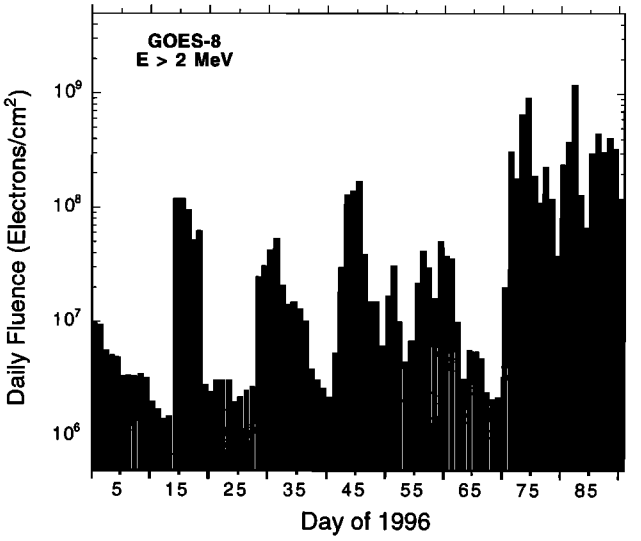

Figure 4. GOES 8 measurements of electrons with E>2 MeV for January to early April of 1996.

that each solar wind stream was associated with a large and relatively brief enhancement of >2 MeV electron fluxes (e.g., in mid-January, in February, and in early March). On the other hand, the strong and complex solar wind variations of late March produced a long-lasting (>2 week) enhancement of relativistic electrons at geostationary orbit beginning on approximately March 12; this persisted until essentially the beginning of April.

Very much the same electron behavior was seen in the data from Los Alamos National Laboratory (LANL) sensors onboard another series of geostationary spacecraft. The data in Figure 5 are for several energy channels onboard S/C 1990-095. The data show that electrons from 0.7 MeV to 6.0 MeV were elevated in association with each solar wind stream in early 1996, but the largest and most persistent flux enhancement was seen from ~day 72 to ~day 92 (12 March to 1 April).

A more extensive examination of the SAMPEX data at low-Earth orbit fully supports the idea that relativistic electrons were substantially enhanced throughout the outer trap-

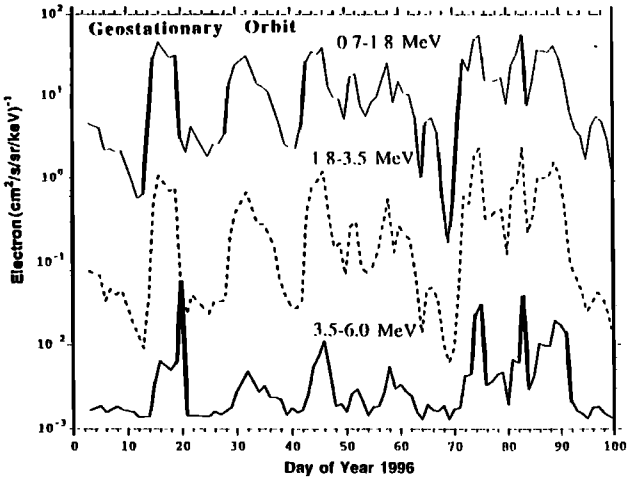

Figure 5. Energetic electron data from LANL instruments aboard spacecraft 1990-095 at geostationary orbit.

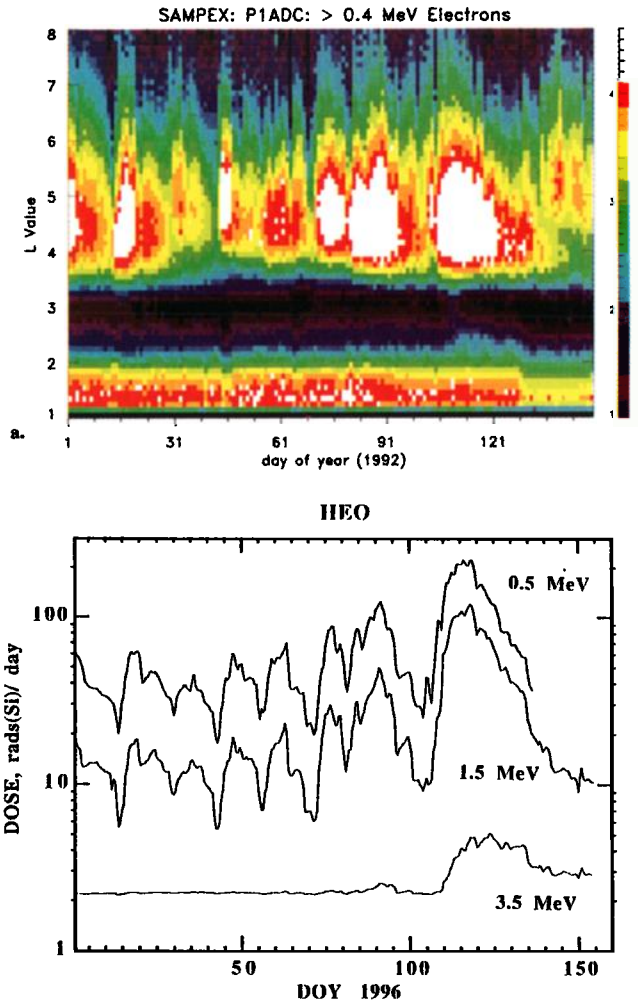

Plate 2. (a) L-sorted SAMPEX electron data for days 1 to 150 of 1996 showing data for the E>0.4 MeV electron channel. The data are color-coded for each day at L=1 to L=8. (b) Data from a dosimeter on a spacecraft in a highly elliptical orbit (HEO) with a 60°-inclination and apogee at 6.6 R_E.

ping zone for nearly 2 weeks in late March. Plate 2a shows color-coded data for electrons with E>0.4 MeV for the period January 1 to April 28 (day 1 to 150). The data are plotted for L=1 to L=8 with the logarithm of count rate shown by the color code to the right of Plate 2. The data are shown as daily averages. It is seen that at each L value, the electron fluxes dropped to very low values around day 70 (~March 10) and then the fluxes increased rapidly thereafter. There was a slight drop on ~day 81 with a persistent climb in flux values after that time until ~day 90. Several strong flux enhancement events were seen in the early part of 1996 and each of these is related to a solar wind stream event. Flux enhancements clearly extend across L values from ~3.5 to L>7.

Plate 2b shows data from a dosimeter onboard a spacecraft at ~60° inclination and having a highly elliptical orbit (HEO) extending out to ~6.6 R_E. Several selected energy channels are used as labeled and the data have been averaged for each day. The period covered is the same (day 1-150) as in Plate 2a. It is seen that the dosimeter showed exactly the same features as the SAMPEX measurements: Each individual brief flux enhancement in January and February looked the same in both data sets. Moreover, the intense and long-lasting flux increases of late March and April of 1996 are also clear. Thus the magnetospheric electron increases are a truly coherent phenomenon.

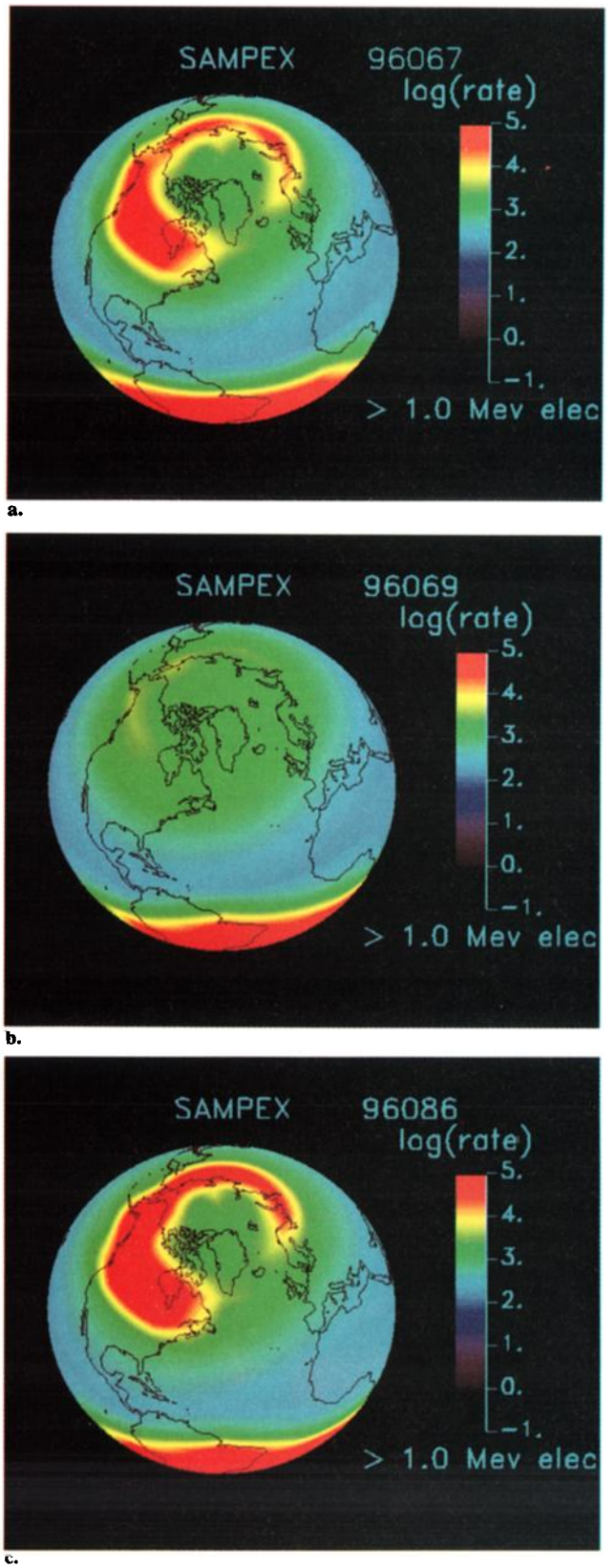

Plate 3. Global image maps of the flux of >1 MeV electrons in the northern hemisphere for selected days in 1996.

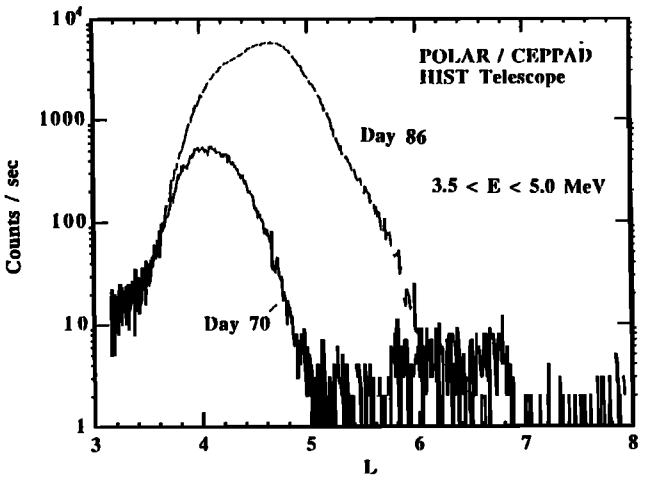

Figure 6. POLAR spacecraft data for high-energy electrons (3.5-5.0 MeV) measured by the CEPPAD/HIST detector comparing March 10, 1996, data with March 26, 1996, data. The spacecraft cuts in L and local time (LT) were similar for these passes. The counting rates are shown versus L value and clearly demonstrate the much higher fluxes and radiation belt width on March 26 compared to March 10. The counting rates can be converted to flux (cm^{-2} -s^{-1} -sr^{-1}) by multiplying by ~10.

The global extent of the radiation belts is shown in a sequence of northern hemisphere radiation belt projection maps in Plate 3. These maps show the count rate of electrons with E>1 MeV measured by the heavy ion large telescope (HILT) sensor on SAMPEX [*Klecker et al.*, 1993] as a function of geographic longitude and latitude. The rather detailed latitudinal measurements and the coarse (16 orbits/day) longitudinal samples are contoured and laid down on a global grid. Plate 3a shows the radiation belt pattern for March 7, 1996. The bright red "collar" around the northern polar region shows that the outer radiation belt was rather intense as a result of a small solar wind stream that peaked on ~March 5. (Note that the red region near the bottom of the image is relatively constant and is due to the South Atlantic Anomaly). Plate 3b shows that the radiation belts, at least at low altitude, had diminished dramatically by March 9 (see Plate 2). After the minimum flux conditions of March 9-10, the flux of trapped electrons strongly recovered. Plate 3c shows that the outer zone was intense and broad throughout late March as is well illustrated by the example shown on March 26, 1996.

A final view of the electron environment in the outer zone is provided by exciting new data from the Comprehensive Energetic Particle Pitch Angle Distribution (CEPPAD) investigation onboard the recently launched POLAR spacecraft [*Blake et al.*, 1995]. The high-sensitivity telescope (HIST) sensor on POLAR measures 0.4 to >10 MeV electrons. In Figure 6, electron fluxes versus L are shown for two similar passes through the outer zone. Data for March 10, 1996 (day 70), were taken when the radiation belts were rather weak. It is seen that HIST channel 11 (covering 3.5 MeV $\lesssim E \lesssim$ 5 MeV) reached a peak counting rate of only ~5×10^2 counts/s. Later, when the radiation belts were much more intense, the flux of electrons measured by HIST was much greater. For example, a similar pass through the radiation belts on March 26, 1996 (day 86) at L values and local times comparable to the pass on March 10 shows that the peak HIST/channel 11 counting rate was ~7 x 10^3 counts/s and the entire outer zone profile was much broader in time. This indicates a much more substantial outer zone electron population on March 26.

Discussion

A number of previous studies [*Gussenhoven et al.*, 1987; *Imhof et al.*, 1991] have considered the temporal changes of high-energy electrons at various points in the magnetosphere. In an early example, *Williams* [1966] found a 27-day periodicity in the variation of electron fluxes ($E \geq$ 280 keV and $E \geq$ 1.2 MeV) throughout much of the outer zone. He ascribed this variation to the effects of high solar wind kinetic pressures and the concomitant high Alfvenic Mach number (M_A^2 is the $\mu_0 \rho V^2/B^2$, where μ_0 is the free space permeability, V is the solar wind speed, ρ is the plasma number density, and B is the interplanetary field strength). *Williams et al.* [1968] subsequently examined the variation of outer zone electrons by using concurrent measurements at low and high altitudes and found closely correlated changes. Later studies examining long-term electron properties tended to focus on available continuous measurements at geosynchronous orbit [e.g., *Paulikas and Blake*, 1979; *Baker et al.*, 1986]. These latter authors also found clear evidence of the strong role of high-speed solar wind streams in controlling the intensity of multi-MeV electrons at 6.6 R_E.

Observations presented in this paper reveal that relativistic electrons increase in absolute intensity, often by a factor of 10 or more, throughout much of the outer magnetosphere on a timescale of order 1 day. These enhancements occur even during quite weak recurrent geomagnetic storm activity. Abrupt flux enhancements might be expected to occur in the very outer magnetosphere, but it is more remarkable that low L shells, deep within the magnetospheric cavity, are able to respond so prominently. As noted above, available solar wind data show that the large electron intensity increases are associated with high-speed solar wind streams impinging upon the magnetosphere. The leading edge of these geo-effective streams have extended regions of southward IMF in front of them.

The present survey of energetic electrons suggests that the outer zone can be divided into several regions based upon the rise and decay characteristics of electron fluxes. Between $L \approx 3$ and $L \approx 5$ the fluxes increase rapidly as the result of a clear geophysical event such as the arrival of a strong solar wind disturbance. About 2 weeks typically pass before a further acceleration event of large magnitude occurs. Outside of $L \sim 5.5$, the magnetosphere is undergoing constant change due to frequent substorm activity. It appears that the region below $L \approx 5$ is populated by occasional strong acceleration events, possibly corresponding to periods of greatly enhanced radial diffusion. The source "turns off" after a relatively short period and the newly energized electron population decays away at a given location. The electron intensities between $L \approx 4$ and $L \approx 5.5$ wax and wane [see *Imhof et al.*, 1991, 1994] and the location of the peak intensity varies in radial distance, indicating that the source mechanisms are able to accelerate a relatively intense energetic electron population on a timescale of ~1 day.

Given the large solar wind speed enhancements and density enhancements (see Figure 4) observed in conjunction with the electron flux increases examined here, we expect large dynamic pressure (ρV^2) enhancements. These pressure increases would compress the magnetospheric field substantially, and in so doing would cause time-dependent (and spatially varying) electric fields. However, the high-speed stream effects would certainly not be as strong as a major shock (and associated storm) nor would the compression occur as quickly. We expect for any substantial inductive electric field associated with the changing B field that some electrons from relatively high L shells would be driven inward by the solar wind stream compression and in the process the relativistic magnetic moment invariant ($\mu_I = P_\perp^2/2m_0B$, where $P_\perp$ is the perpendicular momentum and m_0 is the electron rest mass) would be preserved. Thus the perpendicular relativistic energy increases in proportion to the square root of the local magnetic field strength (B) at the final particle location. However, it would be surprising in this scenario to achieve very high energization due to the relatively slow compressions associated with solar wind streams. We look forward to a future evaluation of this acceleration mechanism.

While the relativistic electrons that are the topic of this paper may still have an unclear acceleration mechanism, their impact on space systems is well known. Scientific satellites (e.g., Spacecraft Charging at High Altitudes (SCATHA) and Combined Release and Radiation Effects Satellite (CRRES)) have simultaneously measured the energetic electron environment and monitored the deleterious effects they can cause on spacecraft electronics. One serious effect is deep dielectric charging which occurs when energetic electrons penetrate and charge dielectric materials. When the fluxes are high enough for a sufficiently long time, the accumulated charge can cause the dielectric to break down, resulting in an electric pulse that can couple into and profoundly disturb critical components. The association between an elevated fluence of relativistic electrons and coincident increases in space system "anomalies" is well established [see *Vampola*, 1987; *Baker et al.*, 1994b].

The practical consequence of relativistic electron modulation in the outer zone is emphasized in the context of the Sun-Earth connection outlined in the present study. It is of interest to note that the Telesat Canada Anik E1 communication satellite located at 111°W at geostationary orbit suffered a severe operational problem on March 26, 1996 [*Danylchuk*, 1996]. The Anik satellite lost all power from its south solar panel array when the array was effectively disconnected from the satellite payload at 2047 UT. The 50% power loss reduced the spacecraft's capacity from 24 C-band channels to nine channels and it reduced the Ku-band capacity from 32 channels to 10 [*Baker et al.*, 1996]. It is not expected that the lost solar panel can be recovered, thus this was a permanent degradation of communication capability for Telesat Canada. It affects a broad range of video, voice, and data services throughout North America. Service to Telesat Canada customers was restored after about 6 hours by link switches to other spacecraft and by using backup systems such as fiber optics ground links [*Roberts*, 1996].

The Anik failure has been determined to be a disconnect of the power distribution unit connecting two batteries to the south half of the solar power array. When recovery from orbit of a failed operational spacecraft is impossible, it is usually difficult to infer an exact cause of failure. Evidence is typically limited to knowledge of the final crucial hardware component that failed, to space environment data collected by other satellites and ground-based systems, and to the listing of anomaly histories of other spacecraft around the critical time [*Allen*, 1994]. It is not clear at this time where, exactly, within the satellite the recent Anik E1 failure occurred. It could have been in the battery system, in the connecting circuitry, or in the solar panel unit itself. The failure mechanism is unclear: It could be a random part failure or related engineering failure. However, it is also conceivable that the space environment may have played a role in the anomaly.

Evidence presented in this report demonstrates that there was a large relativistic electron flux increase during the same period of time as the Anik E1 failure. This suggests a relatively hostile space environment. Several other spacecraft also suffered operational anomalies on, or about, March 26, 1996 [*Baker et al.*, 1996]. Indeed, a remarkable array of scientific and operational spacecraft, as shown here, reveals that the high-energy electron environment was quite elevated throughout late March 1996. The satellite and ground-based data suggest that the space environment could have caused, or at least exacerbated, the conditions onboard Anik E1 that led to the power failure that crippled the spacecraft [*Baker et al.*, 1996] through the mechanism of deep-dielectric charging. As is the case for most on-orbit anomalies, one does not know, and probably will never be able to determine, whether the space environment was a significant factor in the Anik failure. However, we have shown using data from several scientific experiments that the radiation environment was enhanced and should be considered in the anomaly analysis.

Acknowledgments. The authors thank the numerous people who have unselfishly shared their knowledge and data. We gratefully acknowledge Capt. S. Quigley of the 50th Weather Sqdn. Special thanks are given to L. Acton for Yohkoh data and to J. Gurman and J.-P. Delaboudiniere for SOHO data. We also thank members of the SAMPEX, POLAR, WIND, GOES, and various other operational spacecraft teams for unflagging support. This work was supported by NASA grant NAG5-2664. L. F. Bargatze was supported by NASA grant NAS8-40801. The research of G. Rostoker was supported by the Natural Sciences and Engineering Research Council of Canada. Ground-based data from the NOAA-NGDC and from the Canadian Space Agency's CANOPUS network have been especially appreciated.

The Editor thanks S. Watari and another referee for their assistance in evaluating this paper.

References

Allen, J. H., Solar-geophysical data: Comprehensive Report, No. 594, part II, pp. 48-61, Feb. 1994.

Baker, D. N., J. B. Blake, R. W. Klebesadel, and P. R. Higbie, Highly relativistic electrons in the earth's outer magnetosphere, I, Lifetimes and temporal history 1979-1984, *J. Geophys. Res.*, *91*, 4265, 1986.

Baker, D. N., G. M. Mason, O. Figueroa, G. Colon, J. Watzin, and R. Aleman, An overview of the SAMPEX mission, *IEEE Trans. Geosci. Electro.*, *31*, 531, 1993.

Baker, D. N., J. B. Blake, L. B. Callis, J. R. Cummings, D. Hovestadt, S. Kanekal, B. Klecker, R. A. Mewaldt, and R. D. Zwickl, Relativistic electron acceleration and decay time scales in the inner and outer radiation belts: SAMPEX, *Geophys. Res. Lett.*, *21*, 409, 1994a.

Baker, D. N., S. Kanekal, J. B. Blake, B. Klecker, and G. Rostoker, Satellite anomalies linked to electron increase in the magnetosphere, *Eos Trans. AGU*, *75*, 401, 1994b.

Baker, D. N., et al., An assessment of space environmental conditions during the recent Anik E1 spacecraft operational failure, *ISTP Newsl.*, *6*, (2), 8-29, June 1996.

Blake, J. B., et al., CEPPAD, *Space Sci. Rev.*, *71*, 531, 1995.

Blake, J.B., D.N. Baker, N. Turner, K.W. Ogilvie, and R.P. Lepping, Correlation of changes in the outer-zone relativistic-electron population with upstream solar wind and magnetic field measurements, *Geophys. Res. Lett.*, 24, 927-929, 1997.

Cook, W. R., et al., PET: A proton/electron telescope for studies of magnetospheric, solar, and galactic particles, *IEEE Trans. Geosci. Remote Sens.*, *31*, 565, 1993.

Danylchuk, J., "Satellite's solar power failure puts broadcasters on the blink," *Edmonton J.*, March 27, 1996.

Feldman, W. C., et al., Long-term variations of selected solar wind properties: IMP 6, 7, and 8 results, *J. Geophys. Res.*, *83*, 2177, 1978.

Gosling, J. T., D. J. McComas, J. L. Phillips, and S. J. Bame, Geomagnetic activity associated with Earth passage of interplanetary shock disturbances, *J. Geophys. Res.*, *96*, 7831, 1991.

Gussenhoven, M. S., et al., New low-altitude dose measurements, *IEEE Trans. Nucl. Sci.*, *NS-34*, 676, 1987.

Imhof, W. L., H. D. Voss, J. Mobilia, D. W. Datlowe, J. P. McGlennon, and D. N. Baker, Relativistic electron enhancements: Simultaneous measurements from synchronous and low altitude satellites, *Geophys. Res. Lett.*, *18*, 397, 1991.

Imhof, W. L., E. E. Gaines, J. P. McGlennon, D. N. Baker, G. D. Reeves, and R. D. Belian, Relativistic electron flux comparisons at low and high altitudes with fast time resolution and broad spatial coverage, *J. Geophys. Res.*, *99*, 17,421, 1994.

Klecker, B., et al., HILT: A heavy ion large area proportional counter telescope for solar and anomalous cosmic rays, *IEEE Trans. Geosci. Remote Sens.*, *31*, 542, 1993.

Lepping, R. P., et al., The WIND magnetic field investigation, *Space Sci. Rev.*, *71*, 207-229, 1995.

Mayaud, P. N., *Derivation, Meaning, and Use of Geomagnetic Indices*, *Geophys. Monogr. Ser.*, vol. 22, AGU, Washington, D.C., 1980.

Ogilvie, K. W., et al., SWE, A comprehensive plasma instrument for the WIND spacecraft, *Space Sci. Rev.*, *71*, 55-77, 1995.

Paulikas, G. A., and J. B. Blake, Effects of the solar wind on magnetospheric dynamics: Energetic electrons at the synchronous orbit, in *Quantitative Modeling of Magnetospheric Processes*, *Geophys. Monogr. Ser.*, vol. 21, edited by W.P. Olson, pp. 180-, AGU, Washington, D. C., 1979.

Robert, O. L., "Telesat considers leasing capacity after Anik failure," *Space News*, 4, April 1-7, 1996.

Vampola, A. L., The aerospace environment at high altitudes and its implications for spacecraft charging and communications, *J. Electrostat.*, *20*, 21, 1987.

Williams, D. J., A 27-day periodicity in outer zone trapped electron intensities, *J. Geophys. Res.*, *71*, 1815, 1966.

Williams, D. J., J. F. Arens, and L. J. Lanzerotti, Observations of trapped electrons at low and high altitudes, *J. Geophys. Res.*, *73*, 5673, 1968.

(Received July 12, 1996; revised December 12, 1996; accepted January 13, 1997.)